By Jill Dill Pasteris,* Brigitte Wopenka, and John J. Freeman
Department of Earth and Planetary Sciences
Washington University, Campus Box 1169
St. Louis, Missouri 63132-4899

and

Peter G. Brewer, Sheri N. White, Edward T. Peltzer, and George E. Malby
Monterey Bay Aquarium Research Institute
7700 Sandholdt Road
Moss Landing, California 95039

Raman Spectroscopy in the Deep Ocean: Successes and Challenges

INTRODUCTION

The deep ocean is a demanding environment to the analyst, one that contains fine particles of degraded organic matter and is characterized by high pressures (about 360 atmospheres at 3.6 km depth), low temperatures (down to ~2 °C), and a high concentration (3.5 wt %) of corrosive salts. Such conditions make it difficult to analyze *in situ* interesting and important geologic materials and dynamic processes on the ocean floor, such as the fluids and solids that issue from hydrothermal vents, the rocks that are formed by undersea lava eruptions, the skeletons and shells of calcareous animals such as corals and clams, and ice-like clathrates that form when natural gas seeps upward through the ocean-floor sediments and into the water column above. Because some of the phases of interest are not stable once they are brought to the surface and exposed to ambient pressure, temperature, and high oxygen concentration, only an *in situ* analytical technique can enable detailed investigation of the ocean environment.

Raman spectroscopy is well suited to meet some of the challenges of analysis on the ocean floor: the technique is very amenable to materials that reside in an aqueous environment (in contrast to infrared spectroscopy[1]); analysis is possible on solids, liquids, gases, and dissolved species; and modern Raman instrumentation has fiber-optically coupled components that can be encapsulated in pressure-resistant housings for operation underwater.

In the present paper we report on the development, modification, cali-

*Author to whom correspondence should be sent.

bration, deployment, and first successful applications of the deep-ocean Raman *in situ* spectrometer (DORISS), which is based on a laboratory-model laser Raman spectroscopic system from Kaiser Optical Systems, Inc. (KOSI). This paper documents some of the analytical successes to date and discusses some of the challenges that lie ahead.

SCIENTIFIC INTERESTS IN THE SEA FLOOR AMENABLE TO RAMAN SPECTROSCOPY

The selection of the components for the deep-ocean Raman system was determined by the anticipated analytical requirements and challenges posed by our scientific interests. Those interests include the mineralogy of the sea floor and the chemistry of pore water, gas seeps, and sea floor vents. We would like to monitor gas vents for such species as CH_4, CO_2, CO, H_2S, and H_2 and to distinguish speciations that are sensitive to oxygen concentration (e.g., CH_4 vs. CO_2, sulfate vs. sulfide) and pH (e.g., HCO_3^- vs. CO_3^{2-}). We also want to make time- and spatially resolved measurements of the ocean chemistry, e.g., investigate gradients in dissolved gases, such as CO_2, and dissolved aqueous complexes, such as sulfate and carbonate. The concentrations of such species typically are homogeneous and unchanging in the deep ocean. When there are compositional variations and concentration gradients, however, such as may exist around a hydrothermal vent, they are often transient. They need to be recorded quickly by an *in situ* technique, such as Raman spectroscopy, that does not disturb the compositional distribution.

Other interests include the identification of biologically precipitated solids such as elemental sulfur produced by bacteria such as *Thioploca* and *Beggiatoa*,[2] the distinction between the biologically produced $CaCO_3$ polymorphs aragonite and calcite, the identification of various manganese oxide phases, and the investigation of phosphate minerals and deposits on the sea floor. Other solids of interest on the sea floor include the silicates quartz and feldspar, as well as the iron oxides magnetite and hematite.

Another oceanographic interest amenable to Raman spectroscopy revolves around clathrate hydrate phases, which incorporate methane and/or carbon dioxide into their structure. For the past several years, researchers at the Monterey Bay Aquarium Research Institute (MBARI) in Moss Landing, California, have been carrying out experiments related to the ocean sequestration of carbon dioxide.[3–6] The latter research addresses the attempt to develop large-scale strategies to limit the growth of greenhouse gas in the atmosphere by placing it in geochemically stable environments.[7–9] The ocean already absorbs over seven gigatons of fossil-fuel-derived CO_2 per year by uptake from the atmosphere. It is well known that at sufficient pressure (i.e., depth, in the ocean) and at temperatures above (but approaching) the freezing point of water, both natural gas (methane) and CO_2 will interact with seawater to form clathrate hydrate, which is an ice-like phase in which gas molecules are trapped in crystalline cages formed by the H_2O molecules.[10–12] Therefore, for the past several years, researchers at MBARI have been using remotely operated vehicles (ROVs) to release liter-scale amounts of liquid carbon dioxide into the deep ocean, where they have monitored its dissolution, downward percolation into sediments, and formation of clathrate hydrates[3,4] with ROV imaging technology. In future experiments, the newly developed DORISS system will be used to make specific geochemical measurements on the liquid CO_2, the seawater surrounding the CO_2, the nature of CO_2 clathrate hydrates, and the sediments that potentially interact with the CO_2.

THE CHALLENGES

Deployment of the DORISS down to a Depth of 3.6 km. The encapsulation of a Raman spectrometer in a pressure-resistant, water-tight housing and its successful deployment by a remotely operated vehicle (ROV) on the ocean floor are challenging tasks. An ROV is an integrated, unmanned submersible that is connected to the research ship on the ocean surface via a tether containing copper power conductors and fiber-optic cables. An ROV can be lowered through the water column (at a speed of 20–30 m/min) to a depth as great as 10 km and then landed on the deep ocean floor (Fig. 1). The ROV is equipped with lights and video cameras, and its position can be determined to within a few meters via acoustic navigation systems on the research ship. MBARI operates two research ships (*R/V Western Flyer* and *R/V Point Lobos*), which are equipped with two different ROVs (*Tiburon* and *Ventana*). The ROV *Tiburon* measures 3.0 m L $\times$ 2.4 m H $\times$ 1.8 m W and has a maximum weight of 3356.6 kg, including a payload of 499 kg.

The lower part of the ROV consists of a modular tool sled with drawers that carry mission-specific, pressure-resistant, and water-tight payloads and instrumentation, such as the DORISS described here. The ROV has robotically controlled manipulators that are operated by specially trained pilots from the control room in the research ship. These robotic arms, which have a range up to 2 m from the ROV, can be used to precisely move mission-specific equipment (e.g., animal cages) or an instrument (e.g., the probe head of the DORISS) on the sea floor. The position of the DORISS probe head can be manipulated with an accuracy of a few centimeters via the ROV's robotic arm and the skills of the human pilot in the control room of the research ship. Video imaging of the lighted underwater scene enables selection of the sample of interest followed by the proper positioning of the probe head near the sample's surface in order to make an analysis. The video cameras are mounted on the ROV, and images are monitored live by both the ROV pilots and scientists in the ship's control room. The dynamic display of the Raman

spectrum can also be observed live on a dedicated computer in the ship's control room. This real-time feedback helps guide the optimum positioning of the Raman probe head with respect to the target sample. The number of spectral acquisitions and the collection times can be controlled in real time, as in the laboratory, via a 10 Base-T Ethernet link. Raman spectra can be acquired not only while the instrument is stationary on the sea floor, but also during descent and ascent of the ROV.

In April 2002, the DORISS was deployed to the deep ocean for the first time, in the tool sled of the ROV *Tiburon*. Since then, both of MBARI's ROVs have been involved in more than twenty-five additional successful deep-ocean deployments, most of them in Monterey Bay off the coast of California and several of them in the Gulf of California, in Mexico.

Our research team consists of two groups. The engineering development and the oceanographic program were carried out by the group at MBARI; most of the laboratory work was carried out by the group at Washington University in St. Louis. Both groups participated in the initial field experiments in the deep ocean of Monterey Bay.

Specification and Selection of the Core Instrument. DORISS is based on a laboratory-model, laser Raman spectroscopic system from Kaiser Optical Systems, Inc. (KOSI), which is the core instrument. The need for the DORISS to be placed repeatedly at different sites on the sea floor demanded the core instrument to have as few moving parts as possible and the laser to give a stable output under the thermal conditions pertinent to the ocean.

A frequency-doubled Nd : YAG laser operating at 532 nm was chosen (Coherent model DPSS532) because of its stability and its ability to be cooled simply by thermal conduction through the high-pressure housing and via its contained air. In addition, the 532 nm excitation wavelength was selected for its relatively efficient propagation through seawater.

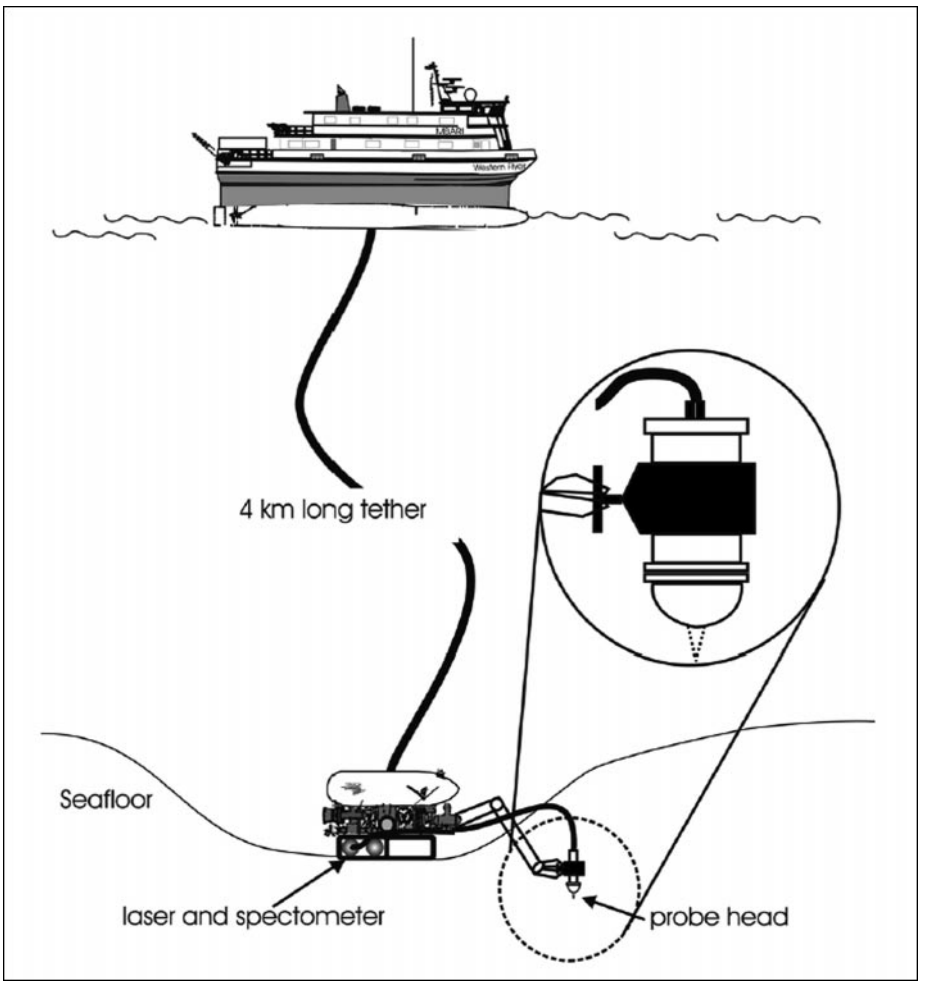

FIG. 1. Schematic overview (not to scale) of the sampling and data-communication systems of the deep-ocean Raman in situ *spectrometer (DORISS) system. The remotely operated vehicle (ROV) is tethered by copper wiring (electrical) and fiber-optic bundles (communication) to the research vessel. DORISS' electronics and spectrometer housings remain in the tool sled of the ROV, whereas the probe head is held by the robotic arm and moved to the sampling site.*

The analysis of the wide range of materials and processes of scientific interest on the sea floor requires a core Raman spectrometer that is physically robust, measures the full spectral range of 100 to 4000 Δcm^{-1}, and has a resolution on the order of 3 cm^{-1}. A wide spectral coverage is required so that data can be collected in the low-wavenumber range (on sulfur and typical minerals, which incorporate inorganic complexes), mid range (on volatiles such as CO_2 and O_2), and high range (for organic compounds, CH_4, and the OH groups of clathrate hydrates and hydroxylated minerals such as zeolites and clays). Appropriate resolution is needed to distinguish mixtures of phases with similar band positions, such as carbonate minerals, and experimentally introduced or natural materials with contrasting isotopic signatures (e.g., ^{12}C and ^{13}C).

Our requirements were met by the following base instrument: Kaiser's HoloSpec f/1.8i spectrometer with a holographic transmissive grating; a front-illuminated charge-coupled device (CCD) camera with 2048 × 512 pixels, by Andor Technology; and Kaiser's Mark II holographic filtered

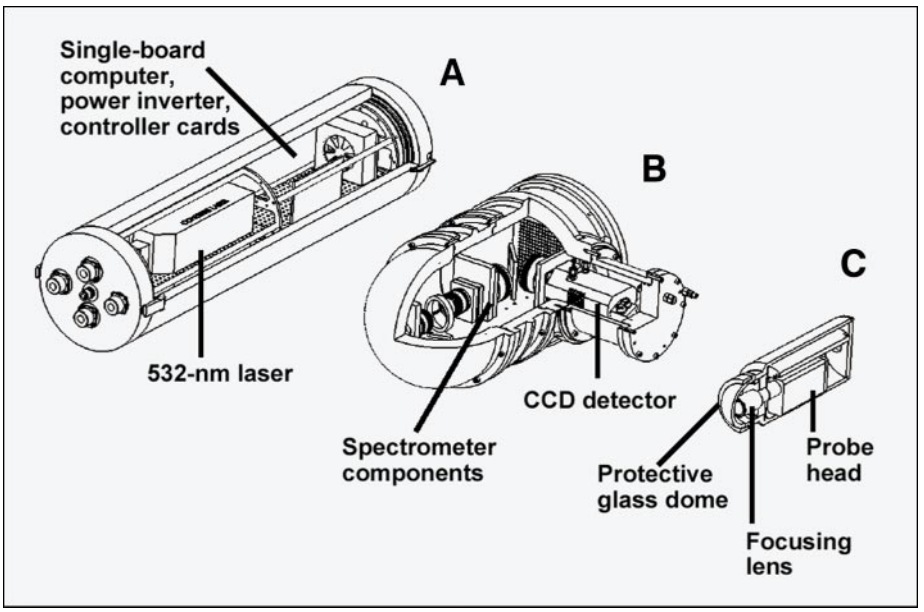

FIG. 2. Schematic view of the distribution of DORISS' components among three pressure-resistant housings: (A) electronics, (B) spectrometer, and (C) probe head. (The handle on the probe head housing and the fiber-optic cables connecting the three housings are not shown here.)

probe head with two interchangeable optical elements: a ''dry'' stand-off optic (i.e., an ~10× objective lens with a focal length in air of ~6.4 cm, which resulted in a maximum working distance of 15 cm when projected through a protective glass dome into seawater); and a short-focal-length immersible optic that consists of an $f/2.0$ lens integrated into the tip of a 25.4-cm-long metal cylinder that is rated for temperatures of −40 to 280 °C and pressures of 0–204 atm.

Making the Core Instrument Seaworthy. The core Raman instrument was reconfigured to permit its deployment in the deep ocean to depths as great as 4000 m.[13] The as-received laboratory spectrometer, plus a single-board computer and power inverter, were re-packaged into three pressure-tight housings: the electronics housing, the spectrometer housing, and the probe-head housing (Fig. 2). The electronics housing holds the Nd:YAG laser, a power inverter (48 VDC to 110 VAC), and a single-board computer with the CCD controller card and flash memory. The spectrometer housing holds the spectrometer, the CCD detector, and the associated electronics. The probe head is contained in a pressure housing with a handle that allows the ROV's robotic arm to hold and move it, thereby bringing the laser into focus on prospective targets. In the case of the dry optic, a ~1.3-cm-thick protective glass dome is used (Fig. 2), through which the exciting laser emerges. This protected dry optic can be used at a depth of several kilometers. For deployment of the DORISS to depths as great as 2000 m, the immersion optic can also be used. The tip of the immersion optic projects directly into the water (this optic not shown in Fig. 2).

An electrical cable connects the DORISS electronics housing to the ROV to provide power and communications via Ethernet protocol through the ROV tether to the surface. For our application, Kaiser and MBARI software engineers developed a remote protocol for controlling the instrument on the sea floor via a computer in the research ship's control room. Two additional electrical cables connect the electronics housing to the spectrometer housing: one connecting the CCD detector to its controller card on the single-board computer, the second providing power and other communications. The probe head is connected to both the laser (in the electronics housing) and the spectrometer via pressure-tolerant fiber-optic cables. The electronics and spectrometer housings remain in the ROV's tool sled during the entire dive (see Fig. 1). The probe-head housing is carried in a tool-sled drawer during descent and ascent of the ROV, but once the vehicle is on the sea floor, the probe-head housing can be picked up and manipulated by the ROV's robotic arm. The translation distance (about 2 m) is limited by the ''arm's reach'' and the lengths of the fiber-optic cables that connect the probe head to the DORISS spectrometer and electronics housings.

The difficulties of cold temperatures and a corrosive, conductive, seawater environment also pose challenges that need to be addressed. Temperature, humidity, and water sensors were installed in the electronics housing and the spectrometer housing to alert the researcher to leaks before serious water damage can occur. Knowledge of the instrument's temperature and other possible instrumental effects is very important for proper interpretation of the spectral data. Packs of desiccant are installed in both the electronics and spectrometer housings to prevent condensation of water vapor onto critical components.

Seagoing instruments are often subjected to significant jostling and vibrations, unlike in a laboratory environment. In addition, between ocean dives, the DORISS typically is removed from its pressure housings and taken apart for inspection, repair, and cleaning. For these reasons, a few components in the original core instrument were removed and replaced with more robust components. These parts included the laser injector and the slit-optimization mechanism. In the latter case, a motorized single-axis stage was installed such that the slit position can be optimized via remote control

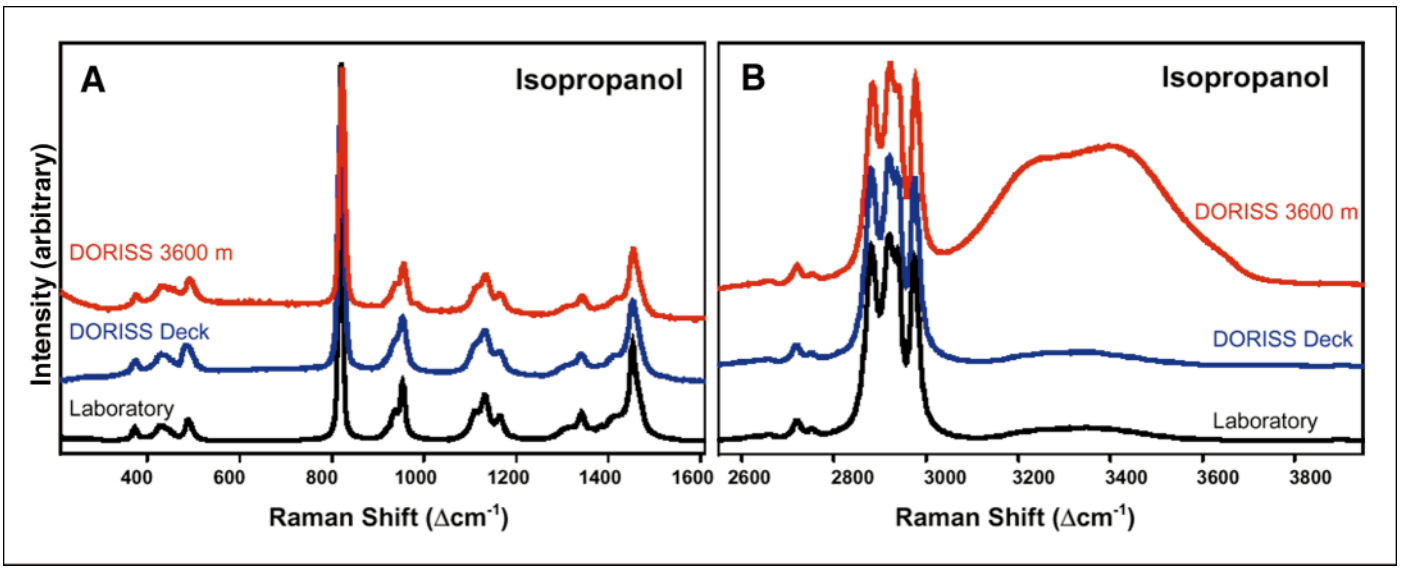

FIG. 3. Comparison of isopropanol spectra acquired with DORISS onboard the research ship in the Pacific Ocean (DORISS Deck), with DORISS at 3600 m ocean depth on the ROV Tiburon *(DORISS 3600 m), and with the duplicate laboratory Raman system at Washington University (Laboratory). Data shown for both* (a) *the low-wavenumber and* (b) *the high-wavenumber spectral regions. For these spectra, a 100 μm spectral slit was used on the laboratory instrument, but no slit was used on the DORISS. The broad double-band feature at 3200–3500 Δcm⁻¹ arises from the intervening seawater.*

while the spectrometer is enclosed in its pressure-tight housing.

EXPERIMENTAL PROTOCOLS

Laboratory Simulations. Many comparison measurements were made with a duplicate KOSI Raman instrument (not enclosed in pressure housings, but with the same laser, gratings, and CCD detector as the MBARI instrument) in the laboratory at Washington University in St. Louis. Simulation experiments were conducted at atmospheric pressure in glass containers. In some studies, we used a 38-liter aquarium tank filled with artificial seawater. The probehead optics were identical to the two types deployed on the DORISS (dry stand-off optic and immersion probe optic), except for the lack of a protective glass dome in front of the dry optic. We analyzed synthetic seawater solutions at temperatures between 2 and 25 °C, mineral samples submersed in water, and gas mixtures contained in glass vessels at ambient pressure and temperature. Even though we were able to simulate the low temperatures appropriate to the ocean floor using a laboratory coolant system, we did not simulate in our laboratory the high pressure that is encountered on the deep ocean floor, i.e., hydrostatic pressures approaching 400 atm at ocean depths of about 4 km.

Calibration Routines. The Kaiser Raman system, like many modern Raman systems, can be purchased with spectral calibration standards (Ne lamp and white light for wavelength and intensity calibrations, respectively) and appropriate software to allow automatic correction of each spectral acquisition for both wavelength and intensity. Such a system works very well under laboratory conditions: the two calibration lamps are used and then a known spectral standard (such as cyclohexane or isopropanol) is analyzed as a so-called ''Raman-shift standard'' to complete the calibration protocol. The unknown samples are run at the same conditions, and the calibration factors (position of the laser line, i.e., 0 Δcm^{-1} on the CCD detector; dispersion of the wavelengths across the pixels of the detector; pixel number vs. intensity response) are automatically applied to the resultant spectra.

Effective calibration in deep-ocean spectroscopy, however, is more complicated. Although it is still possible to carry out a calibration shipboard immediately before the DORISS is lowered into the ocean (the procedure we have been following), the calibration is affected as the instrument moves downward: The decreasing water temperature cools and *differentially* contracts the components of the laser, spectrometer, and CCD detector. Moreover, the pressure-tight housings flex slightly, thereby affecting the physical alignment of the components. Our results suggest that the above factors shift the recorded band positions by several wavenumbers and probably affect the recorded band intensities differently across the spectral window.

For the DORISS instrument, absolute wavelength calibration with a Ne lamp standard is performed shipboard immediately before each dive, which establishes the dispersion function. This is followed by a shipboard ''Raman shift calibration'' (i.e., relative wavenumber calibration) using both a liquid standard (such as isopropanol in a glass vial) and a solid standard (such as diamond). Raman shift standards are

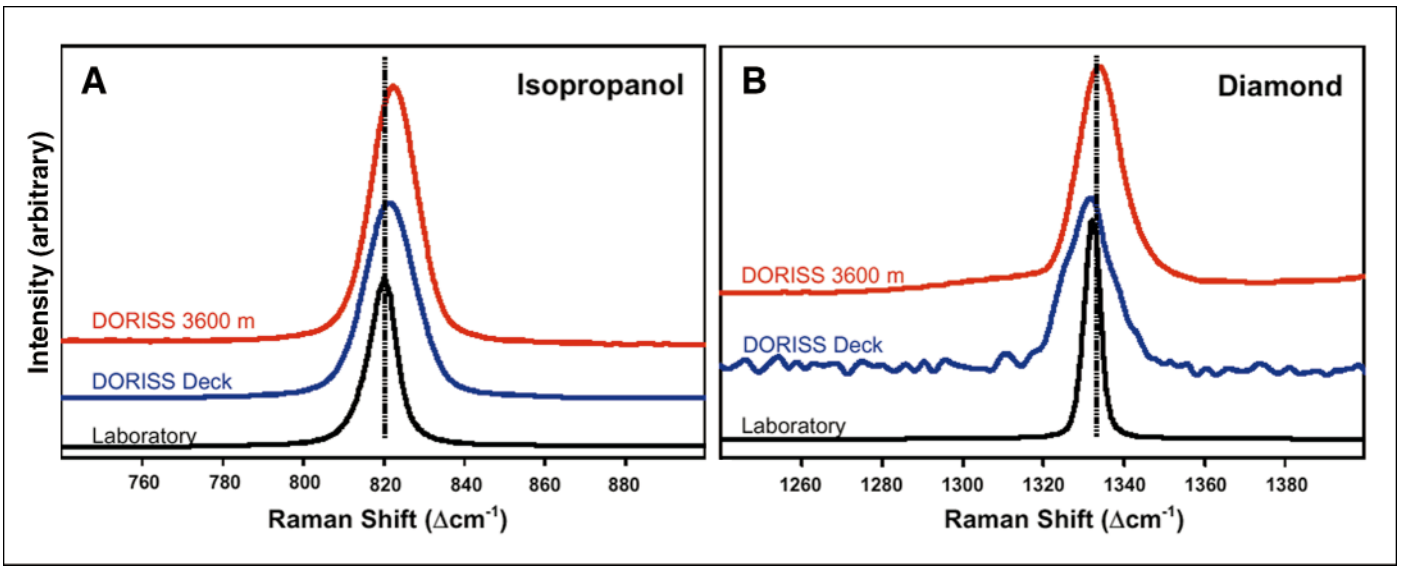

FIG. 4. Comparison of spectral quality and peak positions measured with DORISS and with the well-calibrated duplicate laboratory Raman system at Washington University. (a) *Blow-up of one of the many Raman peaks for isopropanol.* (b) *Blow-up of the only Raman active peak for diamond. The spectra were acquired with DORISS onboard the research ship in the Pacific Ocean (DORISS Deck), with DORISS at 3600 m ocean depth on the ROV* Tiburon *(DORISS 3600 m), and at Washington University (Laboratory). The laboratory instrument had a 100 μm spectral slit, whereas the DORISS had no slit for the acquisition of these spectra.*

used for shipboard calibration immediately before and immediately after each dive.

As an additional aid to monitor and evaluate dive-induced changes in the DORISS instrument's response while submerged, we have placed a small, polished diamond chip *within* the probe head, but considerably away from the focal point of the laser.[14] The extremely strong Raman scattering efficiency of diamond assures that the positioning of a small diamond in the probe head provides continuous monitoring of the diamond's band position as a Raman shift standard, because the 1332 Δcm^{-1} band is superimposed on each spectrum. Because the diamond is within the pressure-tight housing, its Raman peak position is affected only by temperature changes during the dive. In our laboratory, a change in sample temperature from 20 °C (as on shipboard) to 2 °C (as on the sea floor) results in a change of less than 0.2 cm^{-1} in the position of the 1332 Δcm^{-1} Raman band of diamond, as predicted in the literature.[15] The continuous monitoring of the diamond band during a dive therefore provides information on the dive's effect on the spectrometer and aids the post-dive correction of the wavenumber calibration.

In some of our earliest dives, both isopropanol and diamond standards were taken down and measured about once an hour at ambient *in situ* sea floor conditions (Figs. 3 and 4). The isopropanol standard was contained in a pressure-compensated glass vial connected to a deformable plastic reservoir, and the diamond chip was mounted on the outside of the glass vial. On those dives, depth-induced shifts in the band positions were recorded not only for isopropanol and diamond, but also for seawater as a function of its pressure and temperature, and thus its density. The spectra for seawater as a function of depth were obtained by directing the laser as it exits the probe head (which is in the ROV's tool sled) into ambient seawater as the ROV descended and ascended.

For the DORISS ocean deployments conducted during 2002–2003, we determined that the wavenumber calibration is displaced by up to +3.2 cm^{-1} at 3600 m depth and 1.6 °C ocean temperature, with the exact value slightly different for each dive. The spectra shown in the present paper (with the exception of those in Fig. 6) thus have an uncertainty of 3 Δcm^{-1} in accuracy of peak position. Nevertheless, the precision (i.e., reproducibility) of peak positions as measured *in situ* on the sea floor is excellent (0.4 Δcm^{-1}). In the dives during the years 2002 and 2003, the DORISS was calibrated for wavelength only; a sea-floor intensity calibration has not yet been attempted.

Typical Analytical Conditions. The analytical conditions varied somewhat between dives depending upon the laser output power, the Raman scattering efficiency of the sample, the transparency of the water, and the degree of focus of the laser on the sample. The conditions of a typical *in situ* analysis are: 10–25 mW laser power (measured output from the probe head while DORISS is still on deck; subsequent adoption of improved laser injector component permits more constant laser power); 1–15 scans of 1–15 seconds duration are averaged; spectral resolution is 6–8 cm^{-1} when no slit is used (resolution determined by the 100-μm diameter of the collection

optical fiber), but 3–4 cm^{-1} when a 50 μm slit is employed.

The laser typically remains on for the full duration of the dive, i.e., during descent and ascent, as well as while the ROV is residing on the sea floor. The laser appears as a focused green light beam exiting the probe head and can be captured live by the ROV's video cameras and watched by the scientists in the ship's control room (Fig. 5). During acquisition of Raman spectra, the ROV's high-intensity lights are typically turned off so as not to interfere with the acquisition of the Raman signal.

EARLY SUCCESSES OF THE DEEP OCEAN RAMAN SYSTEM

Fluids. ***Raman Spectra of Seawater.*** Among the first spectra obtained with the DORISS were those of seawater. An early concern that did not materialize into a problem was the possibility of a laser-induced high fluorescence background in Raman spectra taken in the deep ocean due to either dissolved organic matter or particulate organic debris (''marine snow'') that constantly rains down through the ocean water column.[16] In practice, however, we found that the fluorescence signal of seawater was not overwhelming and rarely approached in intensity that of the Raman OH stretching bands of water at about 3400 Δcm^{-1}.

The Raman spectrum of (ocean) water (Fig. 6) is characterized by the OH bend and stretch, centered at ~1640 and ~3400 Δcm^{-1}, together with the ν_1 sulfate band (~981 Δcm^{-1}), as has been reported for *ex situ* analysis of natural and synthetic seawater.[17,18] The covalently bonded anionic complex, SO_4^{2-}, which has an average concentration of 28 mM in seawater, is readily recorded (Fig. 6). In fact, our laboratory Raman instrument can detect sulfate in seawater diluted to 0.057 times its normal salinity, i.e., 1.6 mM sulfate or 150 ppm sulfate. Although the purely ionic species such as Na^+ and Cl^- do not yield explicit Raman bands, the nature and concentration of dissolved salts have a measurable effect on the band structure of water.[19–21] This effect is illustrated by the difference in the OH bands of pure water and ocean water, which has 35 g/kg dissolved salts, as shown in Fig. 6.

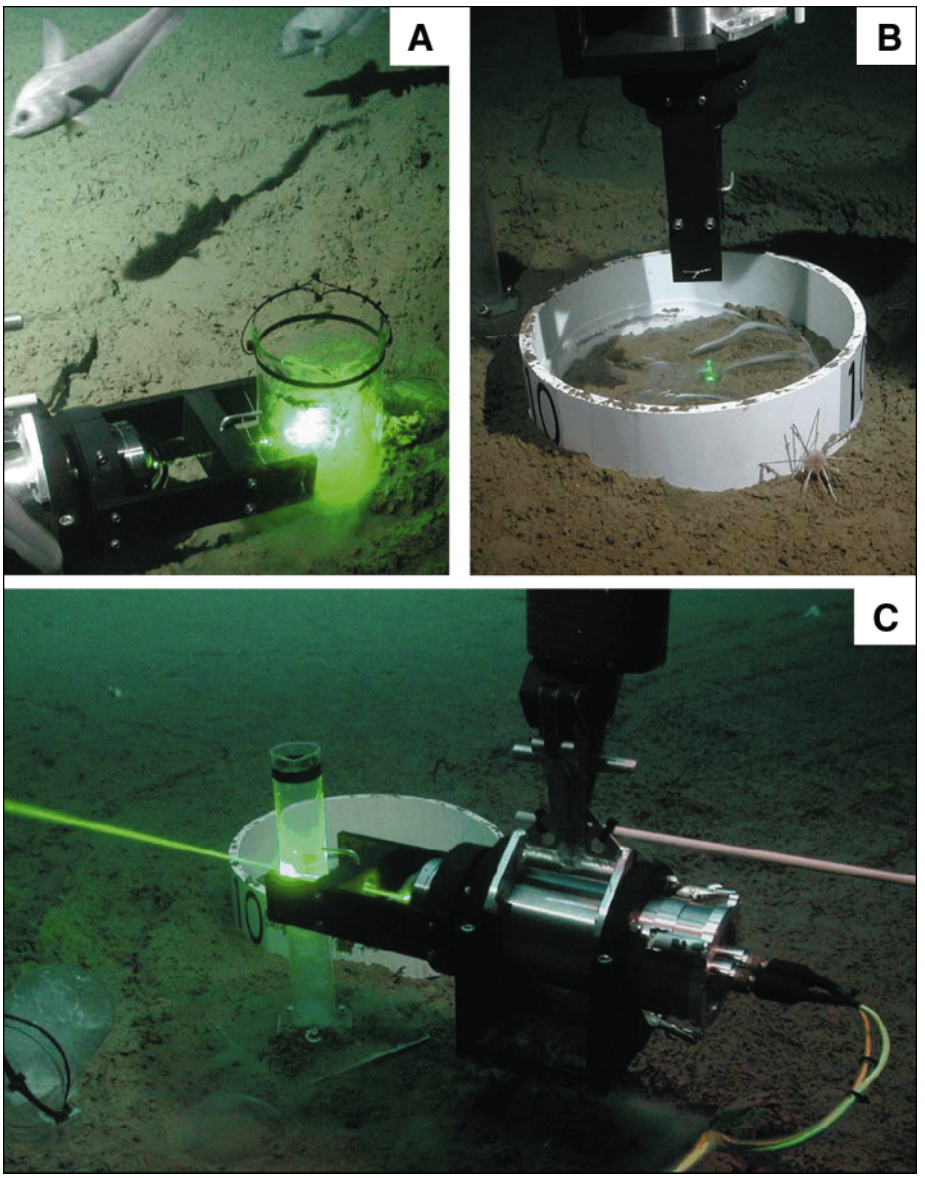

FIG. 5. Laser–sample interaction in three types of experimental configurations during Raman analysis on the deep ocean floor: (a) CO_2–water–hydrate "slush" in a beaker on sea floor; probe head focused horizontally into beaker; (b) probe head focused vertically down onto large, clear blob of CO_2 that almost completely covers bottom of corral; (c) robotic arm (vertical, black) holds probe head and brings the laser into focus on (and through) CO_2–water–hydrate slush in graduated cylinder; large beaker of similar slush lies on its side on ocean floor (bottom, left).

Raman Spectra of Carbon Dioxide Introduced into the Deep Ocean. Raman spectroscopy offers one important means of monitoring the composition of a CO_2 stream that may be introduced into the ocean, e.g., in connection with studies of ocean sequestration of CO_2. In the past, we have done Raman analyses in the laboratory[22] on pure CO_2 enclosed in a glass capillary under controlled conditions of temperature (23

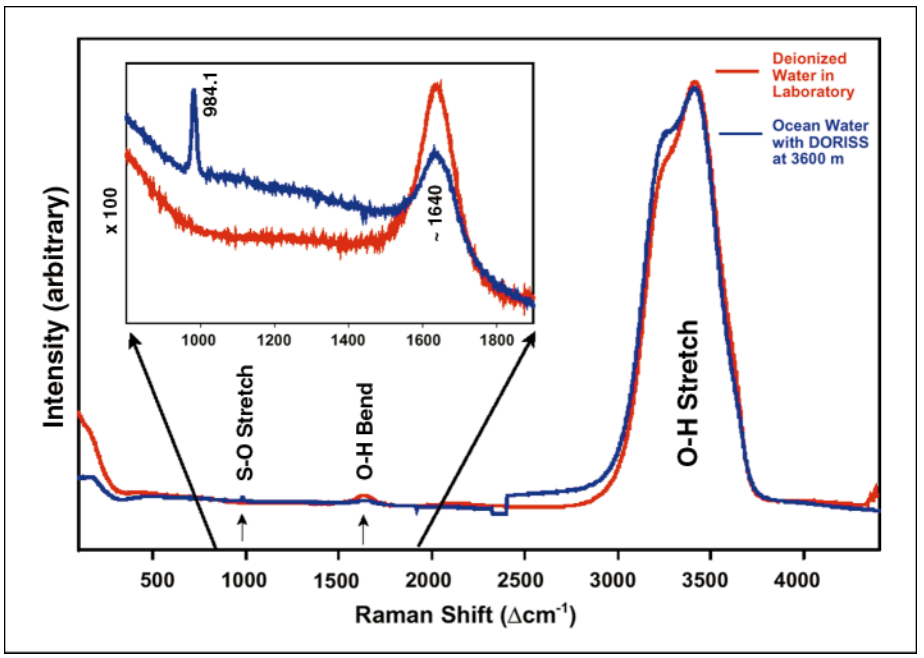

FIG. 6. Comparison of the Raman spectra of deionized water (acquired with the laboratory system at Washington University at room temperature) and ocean water (acquired with the MBARI Deep Ocean Raman System at 3600 m depth and 4 °C). Inset shows enlargement of 800 to 1900 Δcm⁻¹ spectral region. The laboratory system had a 100 μm spectral slit, whereas the DORISS had no slit (resolution imposed by 100 μm collection fiber).

°C) and pressure (up to 700 bars). In April 2002 we used DORISS to make comparable pressure- and temperature-dependent measurements on 500–600 mL (measured in liquid state) of essentially pure CO_2, which were injected underwater into an inverted clear, soft-glass jam jar. (The choice of container was forced upon us by the exigencies of field work.) The jar was mounted within the tool sled of the ROV. The open-ended, inverted jar permitted the CO_2 to equilibrate with both the pressure and temperature of the surrounding seawater as the ROV descended to 664 m depth at 5.2 °C and then returned to the surface. The jar underwent video monitoring during the entire experiment. During the initial descent of the ROV, CO_2 was introduced in several aliquots (beginning at 200 m depth) at increasing depths, as the increasing pressure caused compression of the CO_2 sample. At depths less than 400 m, two phases were observed in the jar: the higher one was a vapor mixture consisting of entrapped air and gaseous CO_2, and the lower one was seawater. At depths of 400 m and greater, there were three phases separated by two interfaces: an upper phase dominated by entrapped air, a middle phase of liquid CO_2, and a lower phase of seawater. Although the density of the CO_2 increased as the ROV moved deeper into the ocean, for the maximum depth of this dive (664 m) and the temperature range of this experiment, the CO_2 phase was always less dense than the seawater and thus remained trapped in the inverted jar.

During the entire descent and ascent, the laser beam was focused into the same small volume within the interior of the jar. At shallower depths, the irradiation volume was at the level of the gas phase; at greater dive depths, the focus was at the level of the liquid CO_2 phase. Raman spectra were taken at a total of 13 intervals (spaced by 40–100 m) along the descent and ascent paths of the ROV. A marked increase in signal intensity and a downshift in Raman band positions for CO_2 accompanied the phase change in CO_2 from the vapor to the liquid state (Fig. 7).

It is well known that the physical parameters of CO_2, such as density and solubility in (sea) water, are a function of temperature and pressure. The ability to monitor changes in these fundamental parameters with the DORISS is important in experiments that test the feasibility of sequestering CO_2 on the ocean floor. The Raman spectrum of CO_2, in turn, is a moderately accurate monitor of its density,[22–30] and Raman spectroscopy can be used to determine the concentration and speciation (e.g., into CO_3^{2-} and HCO_3^-) of CO_2 dissolved in water.[31–33]

Our laboratory work[22] and that of others has shown that, as CO_2 density increases, the Raman band positions of both bands of the Fermi diad[34] downshift, whereas the spectral separation increases between these two bands.[23,25,26] We used the equation of state of Span and Wagner[35] as implemented with the program CO2Tab from ChemicaLogic Corporation[36] to calculate the density of the CO_2 in our previous laboratory experiments[22] and in the ocean experiment. Figure 8 compares the spectral separation between the bands of the Fermi diad as a function of calculated CO_2 density for both our laboratory data and ocean data. The laboratory and DORISS curves are, for the most part, parallel but offset by more than a wavenumber, suggesting that the calibration (specifically the spectrometer dispersion function) applied to the DORISS was not optimal for the conditions during this dive. The marked nonparallelism in the low-density (i.e., low-pressure, shallow-ocean) data suggests that the CO_2 had not come to thermal equilibrium with the surrounding seawater when the spectra were acquired. In such cases, our assumption that the temperature of the CO_2 sample was the same as that of the ambient seawater would have lead to a miscalculation of the density of the CO_2.

In other experiments testing the possibility of ocean sequestration of

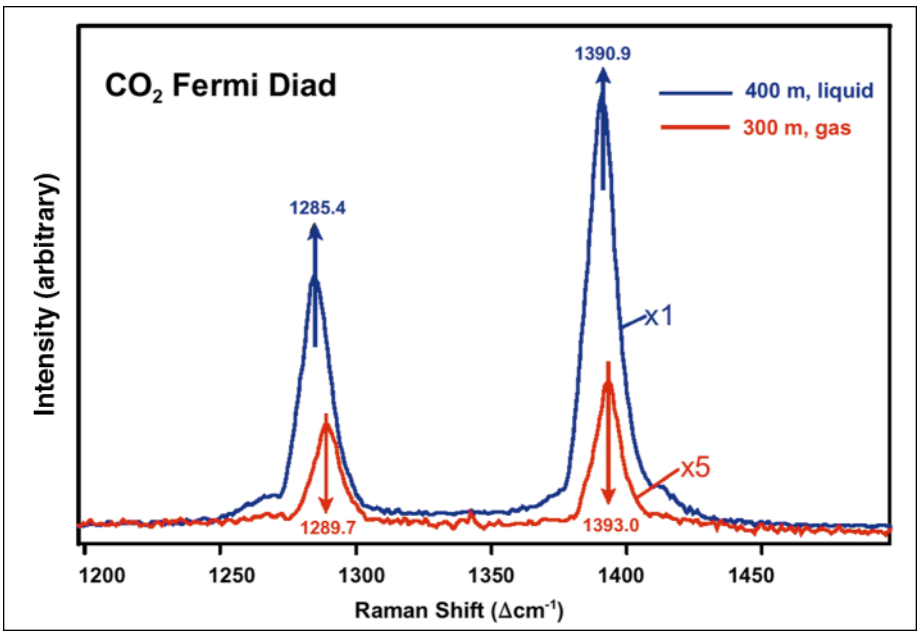

FIG. 7. Raman spectra of liquid and gaseous CO_2 collected during small-scale CO_2 injection experiments on the ROV Tiburon. *Raman spectra were acquired during ascent from the ocean floor while DORISS was sitting in the ROV's toolsled. Difference in phase is recognized by strong increase in intensity and spectral downshift in the liquid compared to the gas. In this figure, the peak positions are uncorrected for depth-induced wavenumber shifts. The spectral separation between the two CO_2 peaks (more accurately measurable than the absolute peak positions) is shown in Fig. 8.*

CO_2, liquid CO_2 was analyzed where it had been deposited at a depth of 3600 m on the sea floor. At these depths, the density of CO_2 exceeds that of seawater, and the liquid CO_2 remains essentially where it was deposited. The Raman probe head was focused into liter-scale immiscible blobs of CO_2, using several different observation geometries (Fig. 5). In some experiments, the laser was projected through the side wall of or directly down onto an open-topped glass vessel into which CO_2 had been injected from the delivery system on the ROV. In other experiments, the laser was projected onto a CO_2 blob placed directly on the sediments of the ocean floor, contained inside of a 50-cm-diameter poly(vinyl chloride) (PVC) ''corral.'' Figure 9 shows a typical spectrum acquired on a CO_2 blob deposited directly onto the ocean floor. The CO_2 bands are superimposed on the background seawater spectrum.

Gases and Their Detection Limits. For our laboratory instrument, we evaluated the detection limits for gas species, based on the use of a stand-off optic with 60 mW of laser power exiting from it. Samples of 1 atm CO_2, 0.7 atm N_2, 0.2 atm O_2, or 0.01 atm H_2O vapor were contained in an Erlenmeyer flask, and the laser was focused through the wall of the glass vessel. We collected 64 acquisitions of 10 seconds each and determined the following detection limits: 0.2 bar CO_2, 0.1 bar N_2, 0.1 bar O_2, 0.01 bar CH_4, and 0.01 bar H_2O vapor. These results are consistent with the well-documented fact that the Raman scattering cross-sections for CO_2, N_2, and O_2 are very similar, whereas the scattering cross-section for CH_4 is almost an order of magnitude greater.[24,37,38] The detection limit for CH_4 is therefore about 10× better than that for CO_2, N_2, and O_2.

The DORISS instrument, enclosed in its pressure-resistant housings, probably has somewhat less sensitivity than the laboratory instrument due to additional signal losses through the pressure-resistant fiber-optic cables, the penetrators through the pressure-resistant housings, and the protective glass dome in front of the stand-off optic. However, even on the maiden voyage of DORISS, operating at a laser output from the head of only 10 mW, we were able to acquire a reasonable spectrum of gaseous CO_2 at 31.33 bars pressure (CO_2 density of 0.077 g/cm^3) in one acquisition of 5 seconds duration (Fig. 10). As will be detailed in a subsequent paper, we have also measured natural occurrences of CH_4 and artificially introduced samples of gaseous CO_2 and N_2 at hundreds of meters depth in the ocean. Moreover, the peak positions of the gases were seen to change with gas density, as predicted theoretically and as determined in laboratory experiments.

Solids. To test our capability in manipulating the probe head into focus on a rock or mineral sample fully immersed in seawater, we strapped several samples of carbonate rocks and carbonate minerals to the outside of a 50-cm-diameter PVC ring and took them to the ocean floor (Fig. 11). In one geometrical configuration, the DORISS probe head projected the laser perpendicular to the approximately 7 × 10 cm face of a translucent, yellow, cleaved rhomb of calcite ($CaCO_3$) affixed to the PVC ring. The ROV operator adjusted the focus of the laser on the calcite by using the robotic arm of the ROV to move the PVC ring. This configuration readily produced a strong Raman spectrum of calcite (Fig. 11b) superimposed on the background spectrum of seawater (not shown).

The superposition of the seawater spectrum does not appreciably degrade the signal-to-noise ratio of spectra taken of minerals on the ocean floor: the positions and strengths of the Raman bands of seawater are such that they do not interfere significantly with the bands of most minerals. The OH stretch bands of many hydrated and hydroxylated minerals tend to be much narrower than and readily distinguished from those of water. In minerals with

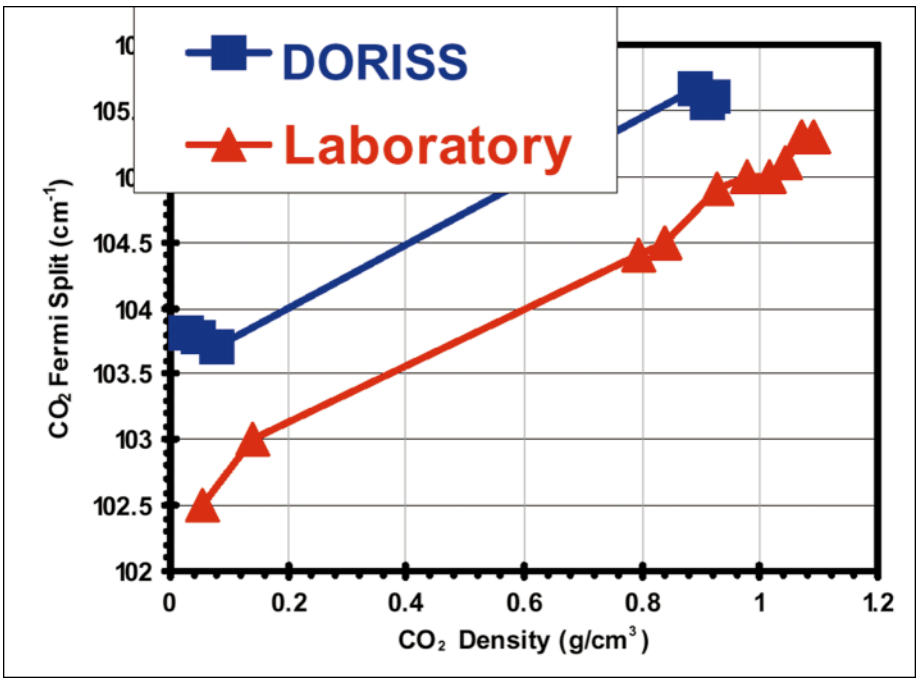

FIG. 8. Plot of the Raman spectral separation between the two peaks of Fermi diad of CO_2 versus CO_2 density (see text). Laboratory data were collected at 23 °C at well-calibrated pressures; Raman peak positions were corrected based on gas emission lines from calibration lamps.[22] DORISS data (uncorrected peak positions) were collected in ascent from 664 m depth in the ocean. Parallelism of laboratory and DORISS data indicates appropriate spectral response to changes in density. Offset between the two curves suggests that the dispersion function that was applied to the DORISS was inappropriate under the specific dive conditions.

weak OH bands, however, the latter could be buried in the strong bands for water.

To date, there has been only one instance in which very high fluorescence precluded useful Raman measurements. This effect occurred when the laser was directed onto clay-rich, organic-rich sediments of the ocean floor, in this case, in Monterey Canyon west of Moss Landing, California. Such fluorescence occurred both during *in situ* measurements and in measurements made in the laboratory on core samples recovered from the same region of the sea floor.

ADDITIONAL CHALLENGES

Selection of Better Calibration Standards. The results of the initial dives in 2002–2003 show that the deep-ocean environment changes not only the position of the 0 Δcm^{-1} on the CCD detector, but also the dispersion of the spectrometer and the intensity response of the integrated system. An *in situ* full calibration protocol is therefore needed during deployment of the DORISS. One possible solution is to incorporate all three calibration sources (Ne lamp, white-light standard, and Raman shift standard) into the pressure-resistant housing of the probe head. This configuration would necessitate additional electronic controls and electro-mechanical devices to bring the calibration sources into and out of the optical path. An alternative and simpler solution in the future might be to use as a wavelength standard the ROV's lights, which typically have been turned off during spectral acquisition. First, however, the Raman band positions and intensities of these lights need to be determined at the temperatures encountered during the deep-ocean calibration.

The selection of Raman shift standards for *in situ* calibration has also been difficult. Such standards (1) should have numerous, narrow bands distributed across the entire 100–4000 Δcm^{-1} region, (2) should be stable and transportable to depth in seawater (if a container is required, it must be transparent to the laser), and (3) either should not be spectrally sensitive to changes in temperature and pressure, i.e., density, *or* should have a very well known spectral response to changes in density. Some liquids that are commonly used in the laboratory as Raman shift standards, such as isopropanol (which we did take to the ocean floor in our first deep ocean dives), are much more compressible than water; this means that they undergo significant changes in density, which can be assumed to be accompanied by significant changes in band positions, making them unreliable calibration standards.

Solid samples such as minerals, in principle, should be better calibration standards than liquids, provided that they exhibit a sufficient number of strong, narrow Raman bands over the spectral range of interest. The diamond standard has been extremely useful in our experiments thus far because the temperature and pressure sensitivity of its Raman band is fully known and because this band lies between those of the Fermi diad of CO_2. We are currently investigating the use of hydrous silicate minerals or polystyrene as a standard. It would be particularly useful if the standard were placed within the housing of the probe head so that only thermal effects would need to be considered.

Improvement of Control on Laser Focus. Laser Raman spectroscopy is a scattering phenomenon that calls for the laser to be focused on a relatively small volume of material in order to create sufficient power density. The same optics used to focus the laser also permit the spatial isolation of the scattering signal. With appropriate optics, one can selectively retrieve the back-scattered radiation and thereby isolate the sig-

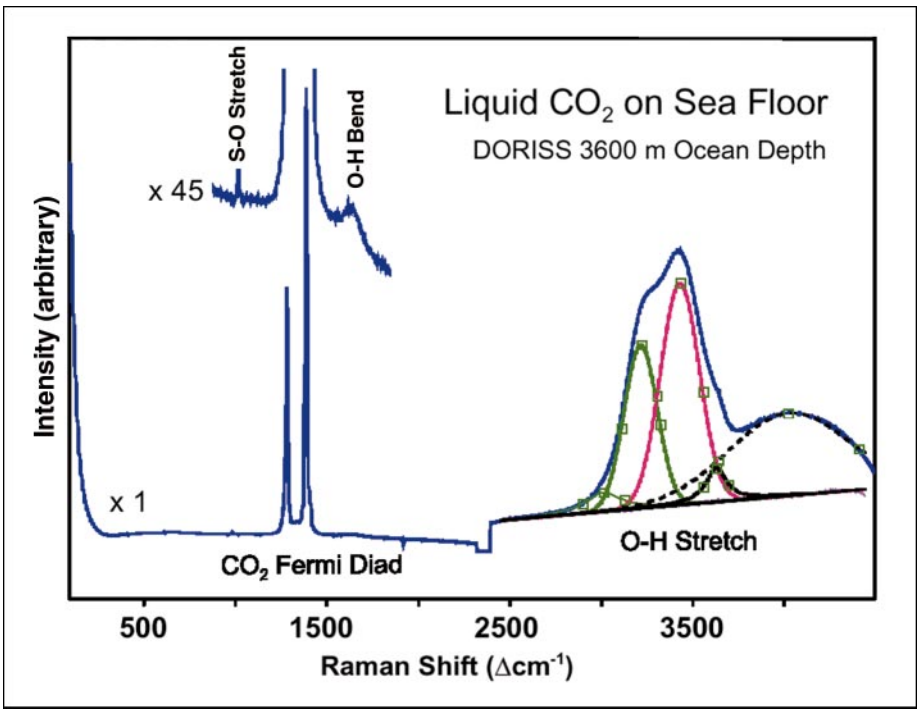

FIG. 9. Raman spectrum taken by DORISS on a large liquid CO_2 blob artificially introduced directly onto the sea floor at 3600 m depth. Although only CO_2 was within the focal volume of the probe head, Raman scattering also was detected from the intervening seawater due to the long focal length of the probe optics.

nal of the desired target from that of its background/matrix.

Whether the Raman spectrometer is configured with a probe head fixed within an optical microscope (in the laboratory) or with a mobile probe head (for sea-floor operation), there are three important issues to consider in the selection of a focusing lens: power-density at the sample, focal length (more specifically, working distance), and depth-of-field. These parameters, of course, are not independent of each other.[39,40] For instance, the power density of the laser irradiation, which is inversely proportional to the size of the focused beam spot, is controlled by the magnification and numerical aperture of the lens.

In our first year of deployments of the DORISS in the deep ocean, the ROV pilot controlled the position of the Raman probe head with respect to the target object through manipulation of the probe head, the sample, or both, by the robotic arm of the ROV. A combination of visual observation of the laser on the sample via the HDTV cameras and the continuous, real-time display of the Raman spectrum recorded by the DORISS system were used when adjusting the sample to improve its focus within the laser irradiation volume (Fig. 12). This type of sample positioning, which can be precise to within several millimeters, depends mostly on the fine-motor skills of the individual pilot who maneuvers the robotic arm of the ROV and the functioning of the arm mechanics at that time. Under these conditions, it is better for the Raman probe head to have a focusing lens that offers a working distance of 5 cm or more to reduce the potential of a collision between the sample and the protective glass dome of the Raman probe head. Large working distances (or focal lengths), however, typically correlate with a large depth-of-field. The latter permits reasonable laser focusing and recovery of the Raman signal even if the distance between the probe head and the sample is difficult to control at the sub-millimeter level. Thus, the $f/2$ lens of the dry optic permitted focus through seawater onto an immiscible blob of carbon dioxide on the ocean floor (Figs. 9 and 12), through a glass beaker into the liquid CO_2 within it, as well as through seawater into a transparent fragment of the mineral calcite (Fig. 11).

Studying samples immersed in the ocean, however, demonstrated two drawbacks to the large working distance (focal length) of the focusing lens that we predominantly have used so far. Firstly, the laser has a long path length through the ambient medium (seawater) before it reaches the target at the laser focal point. Although this surrounding medium is not at the point of laser focus, the seawater does scatter the beam (thereby decreasing the laser intensity on the intended target), and some of that back-scattered light is accepted by the lens. This means that the spectrum of the sample is always superimposed on that of the background (Figs. 3, 9, and 12). Secondly, this spectral superposition eliminates the ability of the Raman probe to spatially resolve compositional differences that occur along the laser beam path, e.g., changes in concentration of dissolved components.

For the above reasons, we have begun testing the use of a high-pressure immersion tip, also with an $f/2$ lens, but with only a 7-mm working distance in water and a small depth-of-field. For purposes of the present discussion, however, we find it more useful to define a parameter called the ''Raman depth of focus,'' which is the distance over which the sample-to-lens distance can be varied while maintaining an intensity of Raman scattering from an opaque sample that is within 50% of the maximum recorded Raman intensity from that sample. By this definition, the immersion lens has a Raman depth of focus of about 0.2 mm in air as compared to about 1.0 mm Raman depth of focus in air for the dry lens. The smaller beam spot (greater focusing) of the immersion lens produces higher signal-to-noise ratios,

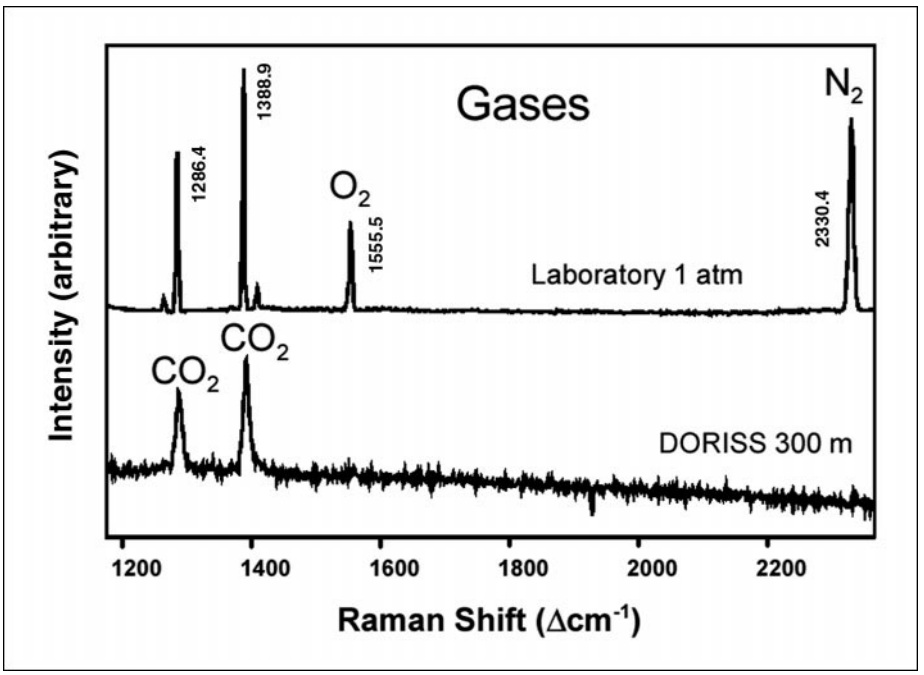

FIG. 10. Raman spectra of CO_2 gas contained at 1 atm in an Erlenmeyer flask in the laboratory (upper trace) and contained in an inverted jam jar in the ocean at 300 m depth (lower trace). Laboratory spectrum also shows signature of air (O_2 and N_2) between flask and probe. Lab spectrum is the average of 64 10-second scans acquired with a 100 μm slit. DORISS spectrum is one 5-second scan acquired without a slit. Small peaks to the low- and high-wavenumber side of the CO_2 Fermi diad are hot bands.[34]

and its shorter focal length produces better rejection of a background seawater signature than does the dry optic. The small Raman depth of focus of the immersion probe is not a problem when the tip is immersed in a gaseous or liquid sample. However, for analysis of an opaque or semi-opaque sample, the immersion lens's smaller Raman depth of focus requires finer control of the sample positioning than is possible with the robotic arm alone.

Another challenge to the focusing capability of the DORISS instrument comes from optical interfaces. Because Raman spectroscopy is a scattering phenomenon, the retrieved signal is affected by all aspects of optical scattering within the sample and on the sample's surface. The case of two transparent liquids with a smooth (although curved) shared interface, as between immiscible liquid CO_2 and water, creates no strong optical problem as long as the laser is aimed perpendicular to the interface (see Fig. 12). Samples that are milky translucent or extremely fine-grained (whether as powders or consolidated solid masses), however, cause almost the same optical responses as opaque phases. This nonpenetration of the interface is due to light scattering, whose intensity

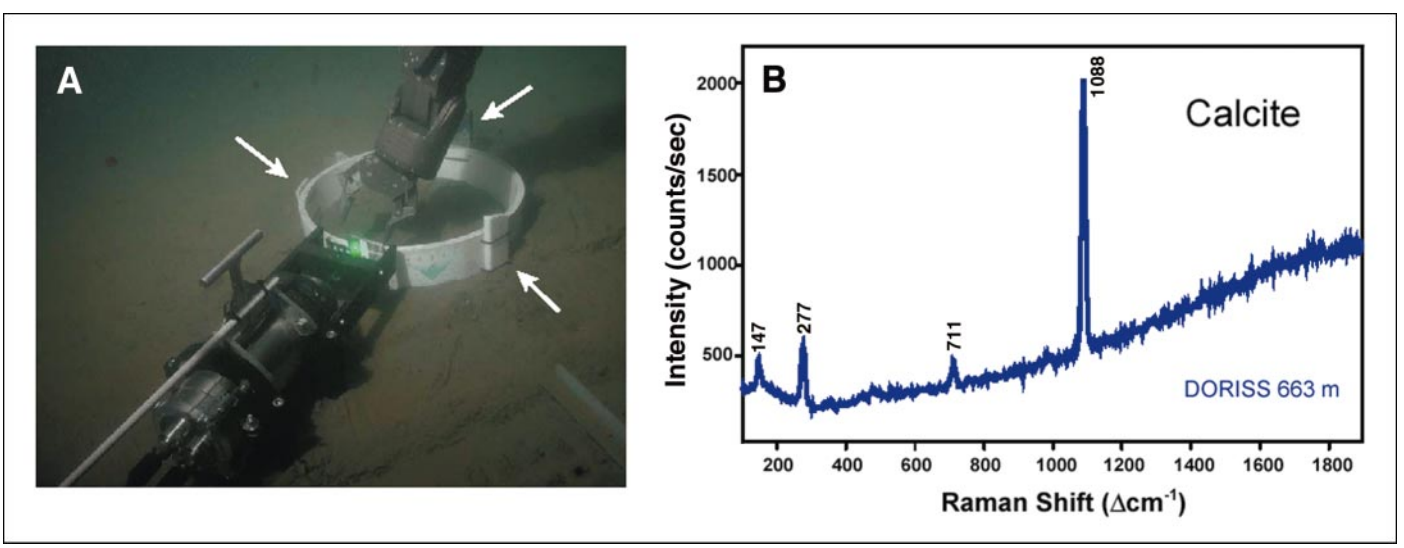

FIG. 11. (a) *Several sawn slabs of calcite and carbonate rocks (indicated by arrows) are strapped to a PVC corral at 663 m depth on the sea floor. The probe head has been guided into focus on the large calcite rhomb painted with a white vertical stripe.* (b) *Raman spectrum of that calcite rhomb (1-second acquisition).*

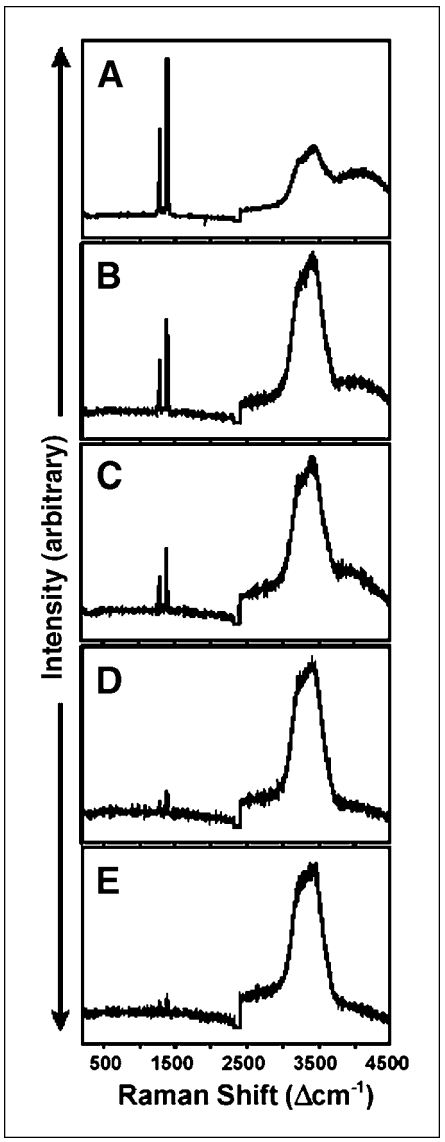

FIG. 12. Series of Raman spectra (each with 1-second acquisition time) as the probe head is moved away from optimal focus of the laser on a CO_2 liquid blob on the ocean floor. As explained in Fig. 9, both seawater and CO_2 are in the laser beam's path. Spectra of both phases are recorded, but the CO_2 : H_2O band intensity ratios vary with position of the probe head. The CO_2 blob is in best focus in spectrum a.

tracks with the difference in refractive index between the two (admixed) substances. Thus, even with the relatively large depth-of-field of the dry optic in its pressure housing, we were unable with the DORISS to obtain a good Raman signal from the fine-grained, milky translucent limestone and marble samples (both rocks are calcium carbonate, i.e., calcite) fixed onto the PVC corral, although the signal from the transparent calcite was very strong (Fig. 11). The same scattering phenomenon apparently prevented us from collecting Raman spectra from the CO_2 clathrate–hydrate polycrystalline mush that formed in some of our experiments.

These optical challenges provided the impetus for additional engineering upgrades to the instrument. We are in the process of testing a newly designed precision underwater positioner, which is a separate, portable platform that can be carried and deployed by an ROV. It is off-loadable onto the sea floor, so as to decouple the probe head from ROV-induced motion or vibration. The positioner is able to place the probe head with an accuracy and reproducibility on the order of 0.1 mm.

Reduction in Weight and Size. The large size and weight of the current version of DORISS make it difficult to transport any additional equipment to the ocean floor when Raman measurements are planned. We therefore are considering both how to reduce the weight of the current base instrument (e.g., by linearizing the optical bench) and whether a different base instrument might be reconfigured to a DORISS instrument. The goal is to make DORISS so small and lightweight that it can be used routinely in conjunction with other types of geochemical and geophysical instruments carried down by the ROV and deployed on the ocean floor.

SUMMARY AND CONCLUSION

We have demonstrated that it is possible to obtain on the sea floor at a depth of 3600 m Raman spectra that have a high signal-to-noise ratio and very good spectral resolution. The main reason that Raman spectroscopy has not been used previously in this environment is that only recently have the following essentials become available: (1) sophisticated carrying platforms such as research ROVs; (2) small, lightweight, portable Raman instruments; and (3) small, stable solid-state lasers. Third-generation Raman spectrometers are now available with holographic gratings, high throughput, and very sensitive CCD detectors that provide the small size and the stability that permitted us to construct the DORISS system.

During construction and implementation of the DORISS, there were many difficulties that needed to be overcome: limitation of size and weight, elimination of fragile optical components, building of housings resistant to pressure and temperature and water, and the establishment of electronic communication and control over a 4-km-long tether from the ship to the remotely operated vehicle and the deep-ocean Raman system.[13]

We have accomplished the first feasibility tests, but we are still in the early stages of solving problems. We have been able to carry out some aspects of calibration (with a diamond chip in the optical path), but we need to improve our methods of both wavelength and intensity calibration. The challenges of precise positioning and focus of the laser have limited our successful analyses to large, transparent objects on the first dives. In response to the needs for accurate laser positioning, focus, and manipulation in the Raman analysis of solid phases (rocks, precipitates, etc.), we are testing a new precision underwater positioning system for measurement of solids in the deep ocean. We also plan to add ''through-the-lens visualization'' to guide our positioning of the laser beam onto the target of interest.

ACKNOWLEDGMENTS

This research was supported by the David and Lucile Packard Foundation and the United States Department of Energy Ocean Carbon Sequestration Program (grants no. DE-FC26-00NT40929 and DE-FC03-01ER6305). We gratefully acknowledge MBARI's Mark Brown for his engineering and design help and Danelle Cline for her skilled work in implementing the software for system operation. The staff of Kaiser Optical, Inc., are thanked for their willingness to provide information necessary to the reconfiguring of the spec-

trometer and its software. We thank the following people for providing carbonate samples that were taken to the sea floor: Bob Cradock, Cheryl Seeger, Jere Cadoret, and Larry Nuelle. We thank the officers and crew of the RVs *Point Lobos* and *Western Flyer*, and the ROV pilot teams of *Ventana* and *Tiburon*, for their skill and support at sea.

1. M. Kraft, M. Jakusch, M. Karlowatz, A. Katzir, and B. Mizaikoff, Appl. Spectrosc. **57,** 591 (2003).
2. J. D. Pasteris, J. J. Freeman, S. K. Goffredi, and K. R. Buck, Chem. Geol. **180,** 3 (2001).
3. P. G. Brewer, G. Friederich, E. T. Peltzer, and F. M. Orr, Jr., Science (Washington, D.C.) **284,** 943 (1999).
4. P. G. Brewer, E. T. Peltzer, G. Friederich, I. Aya, and K. Yamane, Marine Chem. **72,** 83 (2000).
5. M. Tamburri, E. T. Peltzer, G. Friederich, I. Aya, K. Yamane, and P. G. Brewer, Marine Chem. **72,** 95 (2000).
6. J. P. Barry, B. A. Seibel, J. C. Drazen, M. N. Tamburri, K. R. Buck, C. Lovera, L. Kuhnz, E. T. Peltzer, K. Osborn, P. J. Whaling, P. Walz, and P. G. Brewer, Proceedings of the Second Annual Conference on Carbon Sequestration (May 5–8, 2003).
7. C. Marchetti, Climatic Change **1,** 59 (1977).
8. N. Handa and T. Ohsumi, *Direct Ocean Disposal of Carbon Dioxide* (Terra Scientific Publishing, Tokyo, 1995).
9. E. A. Parson and D. W. Keith, Science (Washington, D.C.) **282,** 1054 (1998).
10. E. D. Sloan, *Clathrate Hydrates of Natural Gases* (Marcel Dekker, New York, 1998).
11. B. A. Buffett, Ann. Rev. Earth Planet. Sci. **28,** 477 (2000).
12. M. D. Max, Ed., *Natural Gas Hydrate in Oceanic and Permafrost Environments* (Kluwer Academic Publishers, Dordrecht, The Netherlands, 2000).
13. P. G. Brewer, G. Malby, J. D. Pasteris, S. N. White, E. T. Peltzer, B. Wopenka, J. Freeman, and M. O. Brown, Deep Sea Research Part I: Oceanographic Research Papers, **51,** 739 (2004).
14. X. Zheng, W. Fu, S. Albin, K. L. Wise, A. Javey, and J. B. Cooper, Appl. Spectrosc. **55,** 382 (2001).
15. D. Schiferl, M. Nicol, J. M. Zaug, S. K. Sharma, T. F. Cooney, S.-Y. Wang, T. R. Anthony, and J. F. Fleischer, J. Appl. Phys. **82,** 3256 (1997).
16. F. Azam and R. A. Long, Nature (London) **414,** 495 (2001).
17. J. S. Bartlett, K. J. Voss, S. Sathyendranath, and A. Vodacek, Appl. Opt. **37,** 3324 (1998).
18. M. Becucci, S. Cavalieri, R. Eramo, L. Fini, and M. Materazzi, Appl. Opt. **38,** 928 (1999).
19. T. P. Mernagh and A. R. Wilde, Geochim. Cosmochim. Acta **53,** 765 (1989).
20. K. Furić, I. Ciglenečki, and B. Ćosović, J. Mol. Struct. **550–551,** 225 (2000).
21. J. Dubessy, T. Lhomme, M.-C. Boiron, and F. Rull, Appl. Spectrosc. **56,** 99 (2002).
22. J. C. Seitz, J. D. Pasteris, and I.-M. Chou, Am. J. Sci. **296,** 577 (1996).
23. R. B. Wright and C. H. Wang, J. Chem. Phys. **58,** 2893 (1973).
24. H. W. Schrötter and H. W. Klöckner, in *Raman Spectroscopy of Gases and Liquids,* A. Weber, Ed. (Springer-Verlag, New York, 1979), pp. 123–166.
25. Y. Garrabos, R. Tufe, and R. Le Neindre, J. Chem. Phys. **72,** 4637 (1980).
26. Y. Garrabos, M. A. Echargui, and F. Marsault-Herail, J. Chem. Phys. **91,** 5869 (1989).
27. A. Hacura, Phys. Lett. A **227,** 237 (1997).
28. B. Maté, G. Tejeda, and S. Montero, J. Chem. Phys. **108,** 2676 (1998).
29. Y. Gu, Y. Zhou, H. Tang, E. W. Rothe, and G. P. Reck, Appl. Phys. B **71,** 865 (2000).
30. M. A. Blatchford and S. L. Wallen, Anal. Chem. **74,** 1922 (2002).
31. A. R. Davis, J. Sol. Chem. **1,** 329 (1972).
32. T. M. Abbott, G. W. Buchanan, P. Kruus, and K. C. Lee, Can. J. Chem. **60,** 1000 (1982).
33. A. J. Berger, Y. Wang, D. M. Sammeth, I. Itzkan, K. Kneipp, and M. S. Feld, Appl. Spectrosc. **49,** 1164 (1995).
34. G. Herzberg, *Molecular Spectra and Molecular Structure* (Van Nostrand Reinhold Company, New York, 1945).
35. R. Span and W. Wagner, J. Phys. Chem. Ref. Data **25,** 1509 (1996).
36. Website for ChemicaLogic Corp., Burlington, MA, http://www.chemicalogic.com/.
37. B. Wopenka and J. D. Pasteris, Anal. Chem. **59,** 2165 (1987).
38. J. Dubessy, B. Poty, and C. Ramboz, Eur. J. Mineral. **1,** 517 (1989).
39. I. Newton, *Opticks, or, A Treatise of the Reflections, Refractions, Inflections and Colours of Light* (Dover Publications, Inc., New York, 1979), based on the 4th edition London of 1730.
40. Nikon Corporation website on microscopy, http://www.microscopyu.com/articles/formulas/formulasfielddepth.html.